

First observations of the Cabibbo-suppressed decays $\bar{B}^0 \rightarrow D^+ K^- \pi^+ \pi^-$ and $B^- \rightarrow D^0 K^- \pi^+ \pi^-$

The LHCb Collaboration ¹

Abstract

Using 35 pb⁻¹ of data collected in pp collisions at $\sqrt{s} = 7$ TeV by the LHCb experiment, we report first observations of the Cabibbo-suppressed decays $\bar{B}^0 \rightarrow D^+ K^- \pi^+ \pi^-$ and $B^- \rightarrow D^0 K^- \pi^+ \pi^-$, and measure their branching fractions relative to the corresponding Cabibbo-favored modes, $\bar{B}^0 \rightarrow D^+ \pi^- \pi^+ \pi^-$ and $B^- \rightarrow D^0 \pi^- \pi^+ \pi^-$, respectively. The ratios of branching fractions are:

$$\frac{\mathcal{B}(\bar{B}^0 \rightarrow D^+ K^- \pi^+ \pi^-)}{\mathcal{B}(\bar{B}^0 \rightarrow D^+ \pi^- \pi^+ \pi^-)} = (5.2 \pm 0.9(\text{stat}) \pm 0.5(\text{syst})) \times 10^{-2}$$
$$\frac{\mathcal{B}(B^- \rightarrow D^0 K^- \pi^+ \pi^-)}{\mathcal{B}(B^- \rightarrow D^0 \pi^- \pi^+ \pi^-)} = (9.6 \pm 1.5(\text{stat}) \pm 0.8(\text{syst})) \times 10^{-2}.$$

Decays such as these will be of use to determine the CKM Unitarity Triangle angle γ .

¹Conference report prepared for Beauty 2011, Amsterdam, The Netherlands; contact author: Steven Blusk

1 Introduction

The LHCb experiment is designed to exploit a wide variety of decays containing beauty and charm hadrons to search for new physics. As part of this programme, decays of the type $B \rightarrow Dh$ will be used to measure the weak phase γ in tree diagrams. Any significant deviation between the value of γ measured in these tree diagrams and the value inferred from loop diagrams would constitute evidence for new physics. The current level of precision on γ is in excess of 10° [1, 2], and a precision measurement will require the large statistics expected from LHCb.

To obtain the most precise measurement of γ with a finite data sample, we expect to extend our analyses to include other decays. In particular, the Cabibbo-suppressed (CS) $B^- \rightarrow D^0 K^- \pi^+ \pi^-$ decay can be used in a time-independent analysis [3], and $\bar{B}_s^0 \rightarrow D_s^+ K^- \pi^+ \pi^-$ can be used in a time-dependent analysis, complementary to $B^- \rightarrow D^0 K^-$ and $B_s^0 \rightarrow D_s^\mp K^\pm$, respectively. Such decays could potentially contribute significantly to the γ measurement, because the branching fractions of these decays are expected to be 2-3 times larger than $B \rightarrow Dh$ decays.

In this note, we report first observations of the Cabibbo-suppressed decays $\bar{B}^0 \rightarrow D^+ K^- \pi^+ \pi^-$ and $B^- \rightarrow D^0 K^- \pi^+ \pi^-$ using 35 pb^{-1} of data collected by LHCb. In addition to increasing our knowledge of B decays, they provide a benchmark from data on the expected yields in LHCb for these and other Cabibbo-suppressed decays that are relevant for the γ measurement.

2 Data Selection

Events are selected using the same criteria as discussed in the analysis of the Cabibbo-favored (CF) decays [4]. Assuming a Cabibbo-suppression factor of $\tan^2 \theta_C$, where θ_C is the Cabibbo angle, we would expect about 100 $\bar{B}^0 \rightarrow D^+ K^- \pi^+ \pi^-$ and $B^- \rightarrow D^0 K^- \pi^+ \pi^-$ signal events in our 35 pb^{-1} data sample. Because of this lower signal yield, additional background suppression is beneficial. We reduce combinatorial background by requiring (i) the B candidate transverse momentum to exceed $4 \text{ GeV}/c$, (ii) its vertex $\chi^2/\text{dof} < 5$, (iii) the flight distance χ^2 to be larger than 144 (12σ separation), and (iv) the B candidate's momentum vector to point back to a primary vertex within $60 \mu\text{m}$. The efficiency of these selection criteria is 88% for both $\bar{B}^0 \rightarrow D^+ \pi^- \pi^+ \pi^-$ and $B^- \rightarrow D^0 \pi^- \pi^+ \pi^-$ signal decays, while retaining $\sim 68\%$ and 55% for the combinatorial backgrounds, respectively. In order to ensure that most of the uncertainties in the efficiencies associated with the kinematics cancel, we apply these same selection criteria to the signal and normalization modes.

In addition to the tightened kinematic selections, tighter particle identification (PID) requirements are applied, most importantly on the kaon in the $K\pi\pi$ system to suppress background from the CF decays. We require kaons to have momentum, $p < 100 \text{ GeV}/c$, as this is the region where the RICH detectors provide excellent K/π separation. We use particle identification efficiencies determined from $D^{*+} \rightarrow \pi^+ D^0 \rightarrow \pi^+ (K^- \pi^+)$ calibration data, and B mass sidebands (from data) to guide our choice of PID cut value. The

D^* calibration data is collected in parallel with physics data, and matches the running conditions under which the physics data is collected. We scan across cut values for the difference in log-likelihoods between the K and π hypotheses ($\Delta LL(K - \pi)$) until the expected statistical precision $S/\sqrt{S+B}$ of the signal exceeds 5, assuming an event yield of 100 events prior to applying the PID requirement. Based on this study, we require $\Delta LL(K - \pi) > 8$, which corresponds to an expected $S/\sqrt{S+B} = 5.2$. A slightly higher statistical precision could have been achieved with a tighter PID requirement, but we chose not to use the tighter cut because of the potential for larger systematic uncertainty. We also tighten slightly the PID cut on pions from $\Delta LL(K - \pi) < 12$ to < 10 , which is $\sim 99\%$ efficient.

We do not explicitly require any subset of the Level-0 (L0) or High Level Triggers (HLT). Because the signal and normalization modes are kinematically almost identical, the trigger efficiencies should be equal to first order. The $K\pi\pi$ final state has slightly less phase space, and slightly lower daughter momenta (mostly due to the $p_K < 100$ GeV/ c cut on the bachelor kaon), and we use simulation to assess this relative efficiency.

3 Signal Efficiency

We simulate the $\bar{B}^0 \rightarrow D^+K^-\pi^+\pi^-$ ($B^- \rightarrow D^0K^-\pi^+\pi^-$) decay using a cocktail of intermediate states, which include 50% $K_1(1270)^-$, 36% (36%) higher K^* resonances, 10% (12%) nonresonant, and 4% (2%) from the excited $D_1(2420)$ and $D_2(2460)$. The kinematic efficiencies are summarized in Table 1. The first efficiency, ϵ_{geo} is the geometrical efficiency for all stable daughter particles from the B decay to be in the angular range from 10-400 mrad; $\epsilon_{\text{det}}/\epsilon_{\text{geo}}$ is the fraction of those decays in which all daughters are reconstructible, *e.g.* they are in the acceptance of the vertex detector and the tracking detectors downstream of the dipole magnet; $\epsilon_{\text{trk}}/\epsilon_{\text{det}}$ is the efficiency of reconstructing all the B daughter tracks given that they were reconstructible; and $\epsilon_{\text{sel}}/\epsilon_{\text{trk}}$ is the efficiency of our analysis selection requirements. The kinematic efficiency, ϵ_{kin} is the product of all the previous efficiency components. We see that the signal and normalization modes have very similar efficiencies, as would be expected. The selection and trigger efficiencies are also consistent with being flat across the $M(K\pi\pi)$ mass spectrum from 0.8-3.0 GeV/ c^2 .

To first order, we expect the trigger efficiency to be identical. Using our trigger simulation, we find the efficiencies for the L0 trigger are slightly larger for the $\bar{B}^0 \rightarrow D^+\pi^-\pi^+\pi^-$ mode than the $\bar{B}^0 \rightarrow D^+K^-\pi^+\pi^-$ mode. The ratio of trigger efficiencies, $\epsilon_{\text{trig}}(B \rightarrow D\pi^-\pi^+\pi^-)/\epsilon_{\text{trig}}(B \rightarrow DK^-\pi^+\pi^-)$ is found to be 1.08 ± 0.04 for B^0 and 1.04 ± 0.03 for B^- . The slightly lower L0 efficiencies for the CS modes are a consequence of the $p_K < 100$ GeV/ c requirement for the CS decays.

We also need to evaluate the kaon particle identification efficiency. For the CF decays [4] we found that the bachelor particles' momentum spectra were well reproduced by the simulation. We therefore use bachelor kaons from $B \rightarrow DK\pi\pi$ signal MC events as a good representation of the bachelor kaon kinematics in data. To evaluate the PID efficiencies, the kaon $\Delta LL(K - \pi)$ values from D^* data are reweighted so that the kinematics

Table 1: Summary of efficiencies for decay channels under study, as determined from signal MC simulation. ϵ_{geo} is the fraction of decays in which all daughters are in the angular range from 10-400 mrad; ϵ_{det} , is the fraction of events in which all daughters are deemed reconstructible in both the vertex detector and the tracking stations downstream of the magnet; ϵ_{trk} is the efficiency that all daughters are reconstructed; ϵ_{sel} is the efficiency for the candidate to pass our analysis selection; ϵ_{kin} is the total kinematic selection efficiency, which is the product of all previous columns.

Decay	ϵ_{geo} (%)	$\epsilon_{\text{det}}/\epsilon_{\text{geo}}$ (%)	$\epsilon_{\text{trk}}/\epsilon_{\text{det}}$ (%)	$\epsilon_{\text{sel}}/\epsilon_{\text{trk}}$ (%)	ϵ_{kin} (%)
$B^0 \rightarrow D^+\pi^-\pi^+\pi^-$	13.6 ± 0.1	10.8 ± 0.1	84.9 ± 0.3	10.1 ± 0.2	0.126 ± 0.003
$B^0 \rightarrow D^+K^-\pi^+\pi^-$	14.2 ± 0.1	10.6 ± 0.1	87.3 ± 0.3	9.5 ± 0.2	0.125 ± 0.003
$B^- \rightarrow D^0\pi^-\pi^+\pi^-$	14.2 ± 0.1	15.8 ± 0.1	87.5 ± 0.2	12.1 ± 0.2	0.238 ± 0.005
$B^- \rightarrow D^0K^-\pi^+\pi^-$	14.8 ± 0.1	15.7 ± 0.1	88.1 ± 0.2	11.9 ± 0.2	0.244 ± 0.005

(p , p_T , and η) of the kaons match the kinematics of our signal kaon. In addition, the PID efficiencies have a dependence on the number of tracks in the event, and that is also included. The weighting procedure is first validated on MC simulation using kaons from a MC-generated D^* sample. We find good agreement between the efficiency from the kaons in the signal MC sample and the weighted D^* calibration sample. We then switch to using the D^* calibration sample from data, and find the efficiency of the $\Delta LL(K - \pi) > 8$ kaon PID cut in data is $(80.4 \pm 0.1)\%$. For the loose PID requirement on the bachelor pions, the efficiency is $\sim 99\%$ and the data and simulation agree to within 0.5%, and thus we use the pion PID efficiencies from simulation. The relative efficiency of the PID selection is therefore $1/0.804 = 1.24$ with negligible statistical uncertainty.

4 Backgrounds

We have investigated possible reflections from $\bar{B}^0 \rightarrow D^+\pi^-\pi^+\pi^-$ and $B^- \rightarrow D^0\pi^-\pi^+\pi^-$, into the respective CS channels using data. We take the CF decays that pass the kinematic selections, and evaluate the probability for each of the two correct-charge daughter pions to be misidentified as a kaon. These misidentification rates are evaluated using D^* calibration data, and are binned in p_T and pseudo-rapidity. To test our overall sensitivity to the average misidentification rate, we also repeated the procedure with the misidentification rate doubled. We found that the background peaks above the B mass signal region, is broad, and at a low enough level that it can be absorbed into our combinatorial background description.

Another source of peaking background are the Cabibbo-favored decays, $B \rightarrow DD_s^-$, with $D_s^- \rightarrow K^-\pi^+\pi^-$. This background is expected to contribute about 8-10 events to our signal, and we explicitly veto them by requiring the bachelor $K\pi\pi$ invariant mass is more than $20 \text{ MeV}/c^2$ away from $m_{D_s^+}$. After this requirement, this background is negligible.

In principle, the $B \rightarrow DD^-$, also contributes to the peaking background, however, this decay is suppressed by $\tan^2 \theta_C$ (relative to $B \rightarrow DD_s^-$) and the $D^- \rightarrow K^- \pi^+ \pi^-$ decay is doubly Cabibbo suppressed.

Another potential background to $B^- \rightarrow D^0 K^- \pi^+ \pi^-$ is $B^+ \rightarrow D^{*+} K^{*0} \rightarrow D^0 \pi^+ K^+ \pi^-$. However, this final state can only be produced through an annihilation diagram, and the rate is already limited to be less than 9×10^{-6} [5].

5 Signals in Data

The $\bar{B}^0 \rightarrow D^+ K^- \pi^+ \pi^-$ and $B^- \rightarrow D^0 K^- \pi^+ \pi^-$ invariant mass distributions are shown in Fig. 1; clear signals are observed at the B meson mass. We extract the signal yields by fitting these invariant mass distributions to the sums of double Gaussian signal models and background components. Due to limited statistics, we fix the signal means to the values found in the CF mode fits, while the widths are fixed to 0.94 times the value in the CF modes, as determined from MC simulations. We see that these shapes provide a good description of the mass peaks. The backgrounds are primarily combinatorial, and from $D^* K \pi \pi$. The latter background is expected to be much smaller in $\bar{B}^0 \rightarrow D^+ K^- \pi^+ \pi^-$, and is only clearly seen in the $B^- \rightarrow D^0 K^- \pi^+ \pi^-$ mass spectrum. The yield and shape of the D^* background will depend on the branching fractions and the helicity amplitudes, which are not known. Due to the limited statistics, we describe the low mass region for $B^- \rightarrow D^0 K^- \pi^+ \pi^-$ using the sum of two Gaussian shapes, which generally describe the low mass D^* structures well. Any D^* contribution in the $\bar{B}^0 \rightarrow D^+ K^- \pi^+ \pi^-$ is much smaller, and we neglect this component in our default mass fit. The combinatorial background is described by an exponential. Unbinned maximum likelihood fits are performed, from which we find 79 ± 14 $\bar{B}^0 \rightarrow D^+ K^- \pi^+ \pi^-$ and 122 ± 18 $B^- \rightarrow D^0 K^- \pi^+ \pi^-$ signal events. To evaluate the significance of these signals, we repeat the fit with the signal yields fixed to zero, and obtain statistical significances ($\sqrt{-2\Delta \log \mathcal{L}}$) [6] of 6.6 and 8.0 for the $\bar{B}^0 \rightarrow D^+ K^- \pi^+ \pi^-$ and $B^- \rightarrow D^0 K^- \pi^+ \pi^-$, respectively. Since the systematic uncertainties that affect the yield (discussed below) are at the level of a few percent, we have thus first observations of these Cabibbo-suppressed decay modes.

The invariant mass spectra for the $\bar{B}^0 \rightarrow D^+ \pi^- \pi^+ \pi^-$ and $B^- \rightarrow D^0 \pi^- \pi^+ \pi^-$ normalization modes are shown in Fig. 2. They are fit using the same shapes as described in Ref. [4]. The fitted signal yields are 2067 ± 61 and 1620 ± 55 for $\bar{B}^0 \rightarrow D^+ \pi^- \pi^+ \pi^-$ and $B^- \rightarrow D^0 \pi^- \pi^+ \pi^-$, respectively.

6 Systematic Uncertainties

The corrections and systematic uncertainties are summarized in Table 2. The corrections are multiplicative factors to the ratios of branching fractions. Most of the systematic errors cancel in these measured ratios, as the final states are topologically identical. The ratio of selection efficiencies are obtained from simulation, and include the uncertainty due to finite MC statistics and the $p_K < 100$ GeV/ c cut. For the kaon momentum cut,

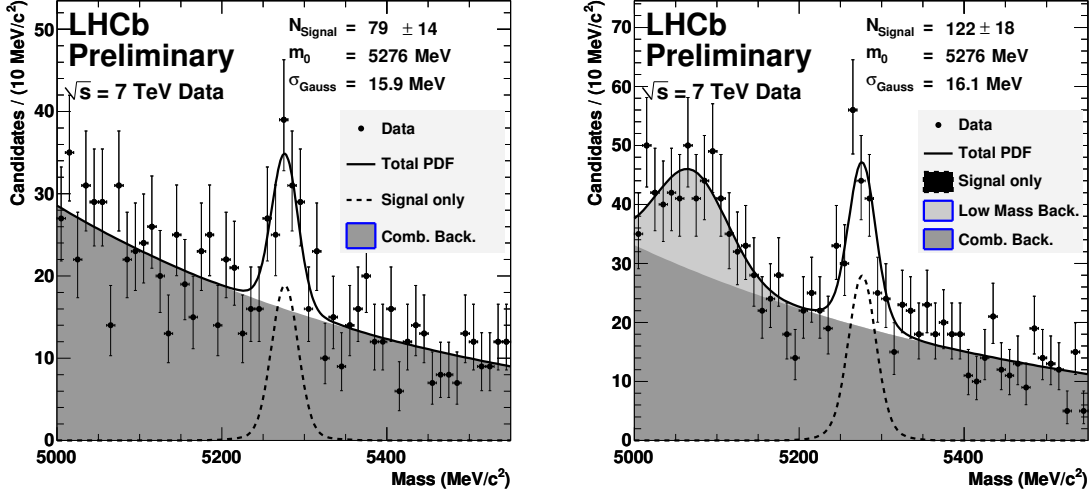


Figure 1: Distribution of the invariant mass for $B^0 \rightarrow D^+ K^- \pi^+ \pi^-$ (left) and $B^- \rightarrow D^0 K^- \pi^+ \pi^-$ (right) candidates from 35 pb^{-1} of data for all analysis selected candidates. A fit, as described in the text is overlaid.

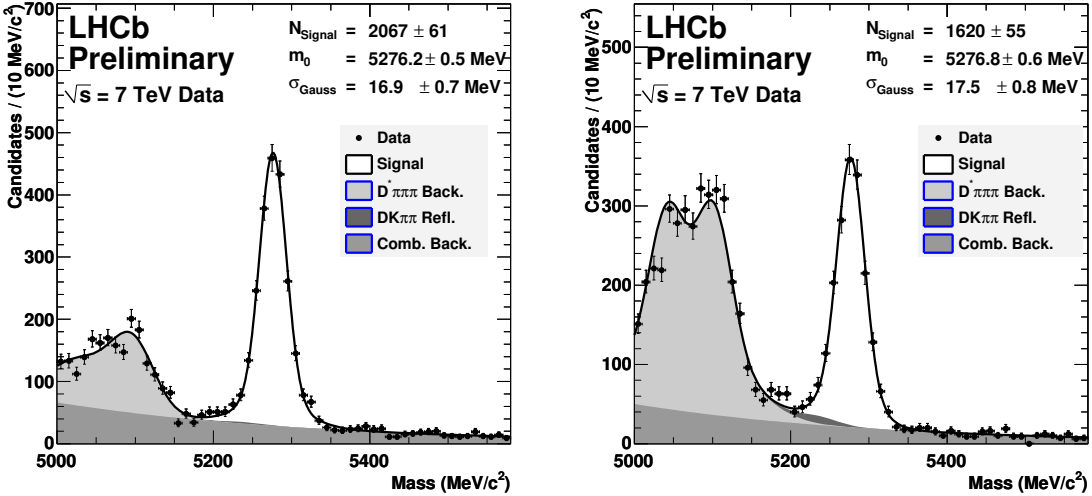


Figure 2: Distribution of the invariant mass for $B^0 \rightarrow D^+ \pi^- \pi^+ \pi^-$ (left) and $B^- \rightarrow D^0 \pi^- \pi^+ \pi^-$ (right) candidates from 35 pb^{-1} of data after applying all analysis selections. The curves are as summarised in the legend and described in detail in Ref. [4].

we have every reason to believe the momentum spectrum is well modelled. For the CF decays, the fraction of bachelor daughters with momentum less than $100 \text{ GeV}/c$ is $(97.0 \pm 0.0.3)\%$ for data and is $(96.7 \pm 0.2)\%$ for simulation (see Fig. 3 in Ref [4].) We therefore conservatively assign a 1% systematic error due to this requirement. We also

must correct for the $\pm 20 \text{ MeV}/c^2$ veto around the D_s^+ mass. This represents about 2% of the $K\pi\pi$ invariant region from 1-3 GeV/c^2 . Since the $K\pi\pi$ invariant mass peaks toward low mass, the fraction of events in this region is certainly less than 2%. We assign the correction to be half of this value, and take the uncertainty as 100% of the correction, or 1.01 ± 0.01 . The trigger efficiency is also evaluated from simulation, and the uncertainty shown is the MC statistical uncertainty. The selection and trigger efficiencies are slightly sensitive to the exact $K\pi\pi$ mass spectrum. To test our sensitivity, we reweight the $K\pi\pi$ invariant mass distribution to double the fraction of events with mass larger than 1.7 GeV/c^2 . We find that the selection and trigger efficiencies change by no more than 1% each. We assume these shifts in efficiency are 100% correlated, and therefore contribute 2% to the total uncertainty.

The kaon PID correction also contributes uncertainty. The reweighting procedure has been tested on MC, and works well. However, we have used signal MC to weight the D^* calibration data, and if the kinematics of the kaon are not perfectly modeled, it could bias the result toward lower or higher PID efficiency. To study this effect, we reweight the $K\pi\pi$ mass spectrum to triple the fraction of events with $M(K\pi\pi) > 1.7 \text{ GeV}/c^2$. This causes a shift in the kaon PID efficiency of 2%, which we assign as a systematic uncertainty. Thus the kaon PID correction is 1.24 ± 0.03 . The efficiency of the tighter pion PID requirement is $\sim 99\%$ efficient in both data and simulation, and is included to first order in our signal efficiency obtained from MC simulation. The associated uncertainty is negligible compared to other uncertainties, and is neglected.

The fitting uncertainty includes uncorrelated errors due to the background descriptions for the signal and normalization mode, and a correlated error due to the signal shape. The combinatorial background descriptions for the CF and CS modes each contribute 2% uncertainty to the yields, as determined by comparing the yields using a linear background model instead of our default exponential background shape. For $\bar{B}^0 \rightarrow D^+K^-\pi^+\pi^-$, our default background shape does not include any low mass D^* structure. To test the sensitivity of our yield to this neglected component, we add a D^* structure with the same shape and relative normalization as observed in $\bar{B}^0 \rightarrow D^+\pi^-\pi^+\pi^-$. Adding this component increases the fitted yield by 5 events, and we include this shift of 6% as a systematic uncertainty in our background model for $\bar{B}^0 \rightarrow D^+K^-\pi^+\pi^-$. The systematic uncertainty in the assumed signal shape is estimated by refitting the CS modes assuming they have equal width to the CF modes (2%). We have also fit the signals with the mean allowed to float, and find that the yields for $\bar{B}^0 \rightarrow D^+K^-\pi^+\pi^-$ and $B^- \rightarrow D^0K^-\pi^+\pi^-$ increase by 1 and 6 events, respectively. Although this is likely to be a statistical fluctuation, we include additional yield uncertainties of 1% and 5%, respectively. We have also assessed the uncertainty in the fits to the normalization modes, and find a systematic error of 2% associated with our understanding of the signal and background shapes. Lastly, based on our previous studies [4], we assign a 2% uncertainty resulting from a difference in the number of multiple candidates in the CF and CS modes. The total systematic uncertainty is therefore 9% for $\bar{B}^0 \rightarrow D^+K^-\pi^+\pi^-$ and 9% for $B^- \rightarrow D^0K^-\pi^+\pi^-$.

Table 2: Summary of corrections and systematic uncertainties to the ratio of branching fractions $\mathcal{B}(\bar{B}^0 \rightarrow D^+K^-\pi^+\pi^-)/\mathcal{B}(\bar{B}^0 \rightarrow D^+\pi^-\pi^+\pi^-)$ and $\mathcal{B}(B^- \rightarrow D^0K^-\pi^+\pi^-)/\mathcal{B}(B^- \rightarrow D^0\pi^-\pi^+\pi^-)$. When one number is given, it is the systematic error alone, with no correction. Corrections are multiplicative.

Quantity	central value \pm syst. error	
	B^0	B^+
Selection efficiency ratio	1.01 ± 0.03	0.98 ± 0.03
D_s^+ Mass Veto	1.01 ± 0.01	1.01 ± 0.01
Trigger efficiency ratio	1.08 ± 0.04	1.04 ± 0.03
$K\pi\pi$ mass spectrum	0.02	0.02
PID efficiency ratio	1.24 ± 0.03	1.24 ± 0.03
CS Background shape	0.06	0.02
CS Signal Shape	0.02	0.02
CS Floated mean	0.01	0.05
CF Mass Fits	0.02	0.02
Mult. candidates	0.02	0.02
Total Correction	1.35	1.31
Total Systematic (%)	9	9

7 Results and Summary

The ratio of branching fractions is given by:

$$\frac{\mathcal{B}(B \rightarrow DK^-\pi^+\pi^-)}{\mathcal{B}(B \rightarrow D\pi^-\pi^+\pi^-)} = \frac{Y(B \rightarrow DK^-\pi^+\pi^-)}{Y(B \rightarrow D\pi^-\pi^+\pi^-)} \times \epsilon_{\text{kin}}^{\text{rel}} \times \epsilon_{\text{trig}}^{\text{rel}} \quad (1)$$

where B (D) is either \bar{B}^0 (D^+) or B^- (D^0), Y are the observed yields, and

$$\epsilon_{\text{kin}}^{\text{rel}} = \frac{\epsilon_{\text{kin}}(B \rightarrow D\pi^-\pi^+\pi^-)}{\epsilon_{\text{kin}}(B \rightarrow DK^-\pi^+\pi^-)}$$

$$\epsilon_{\text{trig}}^{\text{rel}} = \frac{\epsilon_{\text{trig}}(B \rightarrow D\pi^-\pi^+\pi^-)}{\epsilon_{\text{trig}}(B \rightarrow DK^-\pi^+\pi^-)}$$

are the relative selection and trigger efficiencies.

Using Eq. 1, the observed yields, and the corrections and systematic errors from Table 2, we obtain:

$$\frac{\mathcal{B}(\bar{B}^0 \rightarrow D^+ K^- \pi^+ \pi^-)}{\mathcal{B}(\bar{B}^0 \rightarrow D^+ \pi^- \pi^+ \pi^-)} = (5.2 \pm 0.9(\text{stat}) \pm 0.5(\text{syst})) \times 10^{-2}$$

$$\frac{\mathcal{B}(B^- \rightarrow D^0 K^- \pi^+ \pi^-)}{\mathcal{B}(B^- \rightarrow D^0 \pi^- \pi^+ \pi^-)} = (9.6 \pm 1.5(\text{stat}) \pm 0.8(\text{syst})) \times 10^{-2}.$$

It is interesting to compare these results to the ratios $\mathcal{B}(B \rightarrow DK)/\mathcal{B}(B \rightarrow D\pi)$ for B^0 and B^+ . Using the branching fractions from the PDG [5] and the recent LHCb results on $\mathcal{B}(\bar{B}^0 \rightarrow D^+ K^-)$ [7], we find:

$$\frac{\mathcal{B}(\bar{B}^0 \rightarrow D^+ K^-)}{\mathcal{B}(\bar{B}^0 \rightarrow D^+ \pi^-)} = (7.52 \pm 0.66) \times 10^{-2}$$

$$\frac{\mathcal{B}(B^- \rightarrow D^0 K^-)}{\mathcal{B}(B^- \rightarrow D^0 \pi^-)} = (7.6 \pm 0.7) \times 10^{-2}.$$

Our results are compatible with these ratios, although there is some indication of a larger relative rate for $B^- \rightarrow D^0 K^- \pi^+ \pi^-$ as compared to $\bar{B}^0 \rightarrow D^+ K^- \pi^+ \pi^-$. The absolute yield for $\bar{B}^0 \rightarrow D^+ K^- \pi^+ \pi^-$ is $\sim 40\%$ of what is found in $\bar{B}^0 \rightarrow D^+ K^-$, and the yield in $B^- \rightarrow D^0 K^- \pi^+ \pi^-$ is about 25% of the yield observed in $B^- \rightarrow D^0 K^-$. In the future, we expect large yields in these decay channels, and expect that they may contribute significantly to the overall sensitivity of the determination of the CKM Unitarity Triangle angle γ at LHCb.

It is interesting to have a look at the $K\pi\pi$ mass spectrum to see if in any single resonance is dominant. Figure 3 shows the $K\pi\pi$ bachelor invariant mass for B candidates in the signal region ($|M - m_B| < 50 \text{ MeV}/c^2$), and overlaid in green are events in the B mass sidebands ($60 < |M - m_B| < 110 \text{ MeV}/c^2$). For $\bar{B}^0 \rightarrow D^+ K^- \pi^+ \pi^-$, a structure consistent with the $K_1(1270)^-$ is evident, but the structure in $B^- \rightarrow D^0 K^- \pi^+ \pi^-$ structure appears broader and peaks at larger mass. This may be signaling that the $K\pi\pi$ bachelor in $B^- \rightarrow D^0 K^- \pi^+ \pi^-$ has larger contributions from the higher mass excited states, *e.g.* $K_1(1400)^-$, $K^*(1410)^-$, $K_2^*(1430)^-$, etc. Clearly more data will be necessary to get a handle on the contributing resonances.

In summary we have reported the first observations of the decays $\bar{B}^0 \rightarrow D^+ K^- \pi^+ \pi^-$ and $B^- \rightarrow D^0 K^- \pi^+ \pi^-$, and measure their branching fractions relative to the Cabibbo-favored decays, $\bar{B}^0 \rightarrow D^+ \pi^- \pi^+ \pi^-$ and $B^- \rightarrow D^0 K^- \pi^+ \pi^-$. These rates are consistent with the expected $\tan^2 \theta_C$ Cabibbo suppression. The $B^- \rightarrow D^0 K^- \pi^+ \pi^-$ decay could play an important role in the extraction of the weak phase γ . As we collect more data, we expect to observe the decay $\bar{B}_s^0 \rightarrow D_s^+ K^- \pi^+ \pi^-$, which will also contribute to the measurement of the weak phase γ .

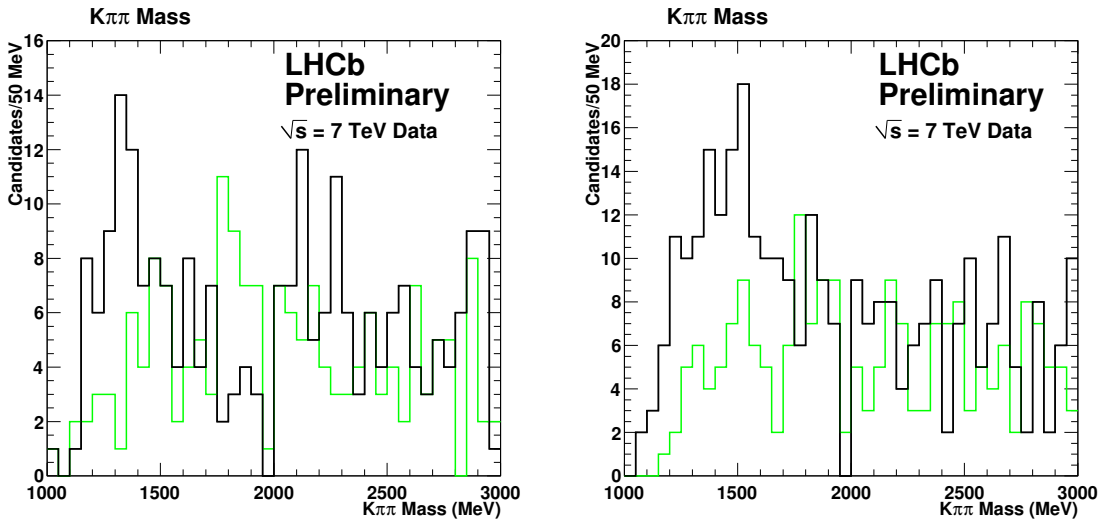


Figure 3: Invariant mass for the $K\pi\pi$ bachelor for $\bar{B}^0 \rightarrow D^+ K^- \pi^+ \pi^-$ (left) and $B^- \rightarrow D^0 K^- \pi^+ \pi^-$ (right). The solid black line corresponds to events selected in the B mass region from $|M - m_B| < 50 \text{ MeV}/c^2$, and the green line shows the sideband region $60 < |M - m_B| < 110 \text{ MeV}/c^2$.

References

- [1] P. del Amo Sanchez *et al.* (BaBar Collaboration), Phys. Rev. D **82**, 072004 (2010); P. del Amo Sanchez *et al.* (BaBar Collaboration), Phys. Rev. Lett **105**, 121801 (2010).
- [2] A. Poluektov *et al.* (Belle Collaboration), Phys. Rev. D **81**, 112002 (2010).
- [3] M. Gronau and D. Wyler, Phys. Lett. B **265**, 172 (1991); D. Atwood, I Dunietz and A. Soni, Phys. Rev. Lett **78**, 3257 (1997) A. Giri, Y. Grossman, A. Soffer and J. Zupan, Phys. Rev. D **68** 054018 (2003).
- [4] *Improved Measurements of the Cabibbo Favored $B_{(s)} \rightarrow D_{(s)}\pi\pi\pi$ and $\Lambda_b \rightarrow \Lambda_c\pi\pi\pi$ Branching Fractions*, LHCb Collaboration, LHCb-CONF-2011-007.
- [5] K. Nakamura *et al.*, J. Phys. G **37** 075021 (2010).
- [6] S. S. Wilks, *The large-sample distribution of the likelihood ratio for testing composite hypotheses*, Annals of Math. Stat. **9**, 60 (1938).
- [7] *Measurement of relative yields of the decay modes $B_d \rightarrow D_{d,s}^+ \pi^\mp$ and $B_d \rightarrow D_{d,s}^+ K^\mp$ and Determination of f_d/f_s for 7 TeV pp collisions*, LHCb Collaboration, LHCb-CONF-2011-013.